31st Congress of the International Council of the Aeronautical Sciences

Belo Horizonte, Brazil; September 09-14, 2018

ENTROPY LAYER EFFECT ON ROUGHNESS-INDUCED LAMINAR-TURBULENT TRANSITION IN SUPERSONIC FLAT PLATE FLOW

Pavel V. Chuvakhov[*,**]
[*]**Central Aerohydrodinamic Institute (TsAGI)**
[**]**Moscow Institute of Physics and Technology (MIPT)**

Keywords: *roughness-induced transition, entropy layer, bluntness*

Abstract

Effect of entropy layer generated by a small leading-edge bluntness on isolated roughness-induced laminar-turbulent transition (RILTT) is studied experimentally at Mach 6 flat plate flow and Reynolds number range (0.46–2.33)×10^6 based on the roughness station. Near-effective cylindrical roughness element of fixed height is considered. Reversal of RILTT with increase of the blunting radius is discussed. The behavior of roughness-induced turbulent wedges is analyzed in terms of boundary layer properties.

1 Introduction

Laminar-turbulent transition (LTT) is a key problem for development of hypersonic flight vehicles and aerospace systems. It is also of principal importance for development of new generation flight vehicles that includes highly economy airplanes with natural or artificial system of laminarization as well as supersonic airplanes with low level of sonic boom. LTT affects sufficiently the aerothermodynamic characteristics of body in flow, e.g. coefficients of viscous friction and heat flux. They have to be known for design and development purposes. LTT depends greatly on the flow conditions and flow disturbances that initiate the transition process. For 'quiet' case of hypersonic flight, irregularities (roughness) of body surface become a possible source of such disturbances.

Leading edges and nose of high-speed flight vehicles must be blunted to prevent them from overheating during the flight. They generate entropy layers of hot low-density gas above the surface. Previous computations and experiments have shown that entropy effect due to rather small bluntness is to drastically reduce heat flux and pressure in regions of shock wave boundary layer (BL) interaction. Entropy layer also damps the growth of Görtler vortexes in the regions of curved flow, e.g. reattachment of compression corner flow, resulting in significant reduction of variations of heat flux due to vortices [1–3].

The summary of roughness-induced LTT in supersonic flows is done in surveys [2, 3]. Investigation of the mechanisms underlying the problem proceeds nowadays both numerically and experimentally. The effect of compressibility is to stabilize the LTT behind the roughness element: the less the Mach number is, the less the transition Reynolds number is. Researchers note that data on RILTT at supersonic speeds are rather limited in Mach and Reynolds numbers. The major part of available data is devoted to the case of sharp leading edge.

There exists very few works dealing with bluntness effects on RILTT [6, 7]. In [6] three large radii of nose bluntness were considered at Mach 10 cone flow with calibrated microspheres installed on its surface. Feasibility of effective turbulization was studied at different roughness stations and angles of attack. It was concluded that the effective sizes of 3D roughness element placed on the cone generatrix line are roughly equal both for sharp and blunt nose cases.

This conclusion was partially confirmed in [7] where Mach 6 blunt flat plate flow at close-to-present experimental conditions. The roughness were calibrated microspheres of six various heights located far away from the leading edge. The bluntness had a cylindrical shape of two large radii (1.6 and 4.3 mm). It was shown

that blunting the leading edge of a plate reduces the required effective roughness Reynolds number. However, the required ratio of effective roughness height k to boundary-layer thickness δ_k at roughness location was essentially constant for both sharp- and blunt-leading-edge plates, being from 1.5 to 3.0. The required value of effective roughness height was shown to decrease with increasing unit Reynolds number for blunt-leading-edge plates. This parameter was found to be essentially constant with varying unit Reynolds number for sharp-leading-edge plates. The Potter & Whitfield [8] method turned out successful for correlation of sharp and blunt leading edge plates.

The both works [6, 7] dealt with relatively large bluntness radii for which the undisturbed boundary layer was well inside the entropy layer.

The present paper aims at extending the blunt-leading-edge data on roughness-induced transition in the Mach 6 flat plate flow. The bluntness effect on nearly effective roughness element is studied at different Reynolds numbers. The present study continues the work reported in [9] that focused on the case of sharp leading edge and roughness element of variable height.

2 General information on the experiments

A test model is a the flat plate of 320×150 mm shown in Fig. 1. There is a thermal insulating insert of plexiglas flash mounted in the top of the steel frame 3 to allow heat flux measurements. The model design allows using exchangeable leading edges of different blunting shapes. The thickness of the sharp leading edge tip 20±1 μm. Its upper surface is of 17 mm long. Geometry of a blunt leading edge is obtained from that for the sharp leading edge by cylindrical conjugating its top and bottom planes that are inclined at 20° to each other. The blunting radii from 0.3 to 2.0 mm are used. The leading edge connects tightly to the plate frame 3 forming a single plane with it. The possible imperfection of the connection is uniform in spanwise direction and is designed to be an upward-facing step of height less than 10μm. Such step is at the bottom of the boundary layer for the present experiments and does not affect the flow, because the corresponding value of Re_{kk} for the step is well under 25 [5]. There are side walls preventing the flow from the bottom of the model.

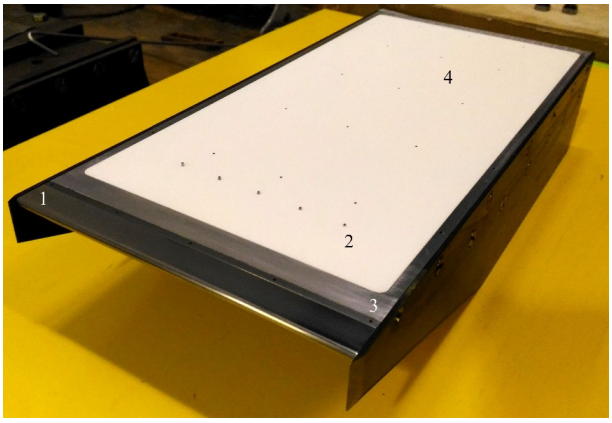

Fig. 1. Experimental model

Five holes are drilled at x_k=60 mm downstream from the leading edge making possible simultaneous measurements for different roughness height. Steel roughness elements of straight cylindrical shape at 20 mm apart from one another are able to protrude above the surface through the tight fitting holes. The present work deals only with the central roughness protruded to the height of 1 mm. It is located well outside the Mach cones from the side corners of plate leading edge even for Mach number approx. 3 at the upper edge of boundary layer, which is relevant to the flow in case of large blunting radius. To make a roughness element protrude to a given height, microscrew of pitch 0.5 mm is toughly connected to each roughness element from the bottom. Rotating the screw with a step 45°, one may achieve a given roughness height with 5° possible overall deviation of the screw angle.

All experiments have been carried out in the shock wind tunnel UT-1M facility (TsAGI) at Mach 6, stagnation temperature T_0=(555±5) K and in the range of Reynolds numbers $\mathrm{Re}_{xk} = \mathrm{Re}_1 \times x_k = (0.46\ldots2.33)\times10^6$, which corresponds to unit Reynolds number range from 7.6×10^6 to 38.9×10^6 m^{-1}. Dynamic viscosity coefficient is computed in accord with Sutherland's law. The Reynolds number varies by changing the stagnation pressure approx. from p_0=10 to 60 bar. All experiments may be split into four different groups with close Reynolds number within each group (see Table 1 for details).

The wind tunnel operates in Ludwig scheme. The Mach 6 profiled nozzle with the exit

diameter of 500 mm follows a lengthy heated high-pressure channel. A single run duration is about 40 ms, for which the flow has nearly constant characteristics in the test chamber.

Table. Grouping of the experimental conditions according to the Reynolds number

Group label	Re_{xk}
#1	$(4.57\pm0.71)\times10^5$
#2	$(8.53\pm0.64)\times10^5$
#3	$(16.63\pm0.79)\times10^5$
#4	$(23.35\pm0.79)\times10^5$

The regions of laminar and turbulent flow are determined using panoramic patterns of heat flux distribution over the entire flat plate surface. Such a distribution is resulted from the thermal measurements of a surface temperature rise for the run time by making use of temperature sensitive paints (TSP) developed in TsAGI. With known measurement timing, properties of thermal insulating insert (item 4 in Fig. 1), wall temperature and flow conditions, one can derive a heat flux from the flow to the surface and express it in the form of dimensionless heat flux coefficient (Stanton number) [10]:

$$\mathrm{St} = \frac{q_w}{\rho_\infty u_\infty c_p \left(T_0 - T_w\right)}, \qquad (1)$$

where subscripts '∞', '0' and 'w' mark values at free-stream, stagnation and wall conditions, respectively.

3 Results

This section describes the results on RILTT for a roughness element that has been effective (Re groups #3, #4), near-effective (#2) or supercritical (#1) (see Table and [9] for details).

To determine laminar-turbulent transition station, a distribution of $\mathrm{St}(x,z_0)$ is considered in log-log scale. Figure 2 shows an example of such distribution on the smooth sharp plate in the middle section $z_0=0$. Nearly linear dependences take place both for laminar, transitional and turbulent branches of the curve. The appropriate dashed red lines are obtained by linear regression of the branches in log-log plane. Their crossing determines the LTT onset and end stations.

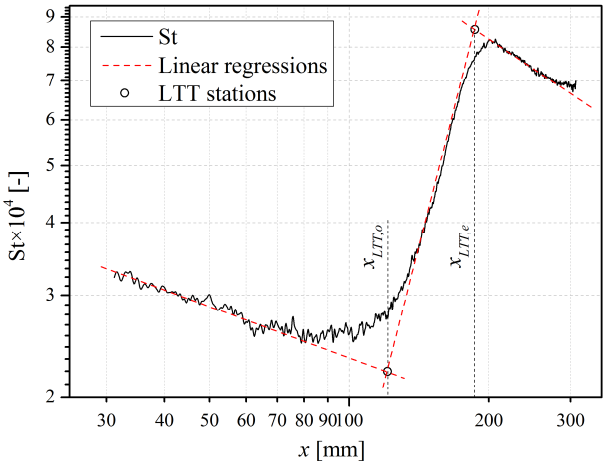

Fig. 2. Definition of LTT onset / end stations; R=0.0 mm, z_0=0, $Re_{\infty,1}=27.5\times10^6$ m^{-1}

To determine the turbulent wedge apex, a $\mathrm{St}(x,z_r+dz)$ distribution is considered in a similar manner, where z_r is a roughness spanwise station. The displacement dz corresponds to the border of the wake. It is intended to move away from the wake core, thereby avoiding the vortex-related influence on heat transfer (see [9] for details).

3.1 Smooth flat plate with bluntness

LTT on a smooth wall is quite sensitive to the value of blunting radius. Its increase pushes LTT downstream unless the onset point goes beyond the plate trailing edge. The transition reversal phenomenon has not been observed for Re groups #3 and #4 and for blunting radii under consideration. Figure 3 illustrates this fact in the plane $Re_{tr,o}$ vs. $Re_b=\rho_\infty u_\infty b/\mu_\infty$, $b=2R$, where subscript 'tr,o' stands for LTT 'onset'. Note that no natural transition has been detected for all the blunting radii in case of Re groups #1 and #2.

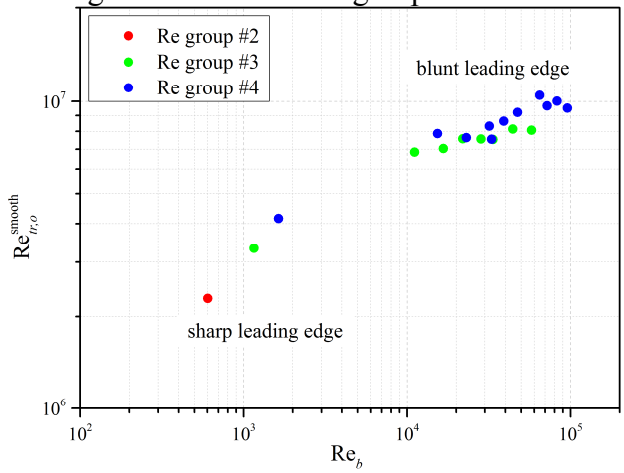

Fig. 3. LTT onset on the smooth plate

In order to ensure the validity of the present results, a correlation due to Simeonides [11] is used to compare the smooth and roughness LTT data. Figure 4 shows a good coincidence of the present data on the smooth wall (closed symbols) with the 'road' from [11].

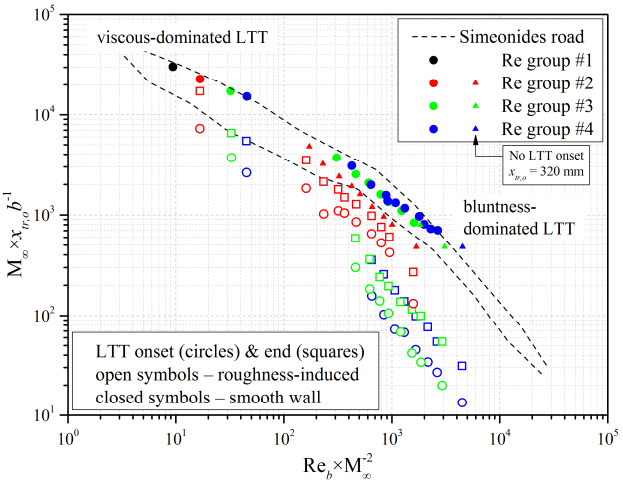

Fig. 4. Comparison of the present data with correlation due to Simeonides [11]

The open points that correspond to roughness-induced transition appear under the road as would be expected. In accord with [11], present data for sharp leading edge case are related to viscous-dominated LTT, while those for all blunted leading edges correspond to bluntness-dominated LTT.

3.2 Visualization of St

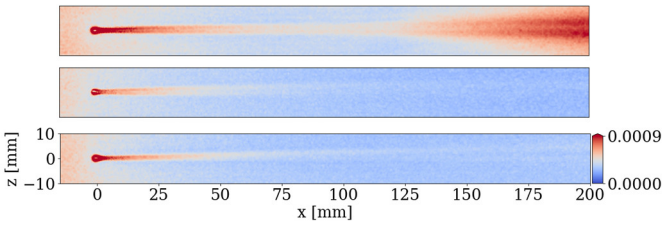

Fig. 5. Distribution of St over the plate surface behind the roughness element (Re group #1, see Table). Blunting radii from top to bottom: 0.0, 0.3, 2.0 mm

In case of the lowest Reynolds number (#1), blunting the leading edge turns the supercritical roughness element into the subcritical one independent on the bluntness radius. Figure 5 illustrates this fact by distribution of St number over the plate surface (x-coordinate is roughness-centered only for Fig. 5–8 and related to the sharp leading edge station for the others). The turbulent wedge disappears even in the presence of the smallest bluntness under consideration.

Near-effective roughness element of Re group #2 'loses' its effectiveness behind blunt leading edge. Figure 6 illustrates this fact: the apex of the turbulent wedge moves fast downstream until R=0.8 mm. For the larger radii, the trend reverses and the apex moves upstream toward the roughness element. One may note the roughness wake becomes stronger as R increases. This is coupled to the fact that roughness height-to-boundary layer displacement thickness increases (see next subsection for details).

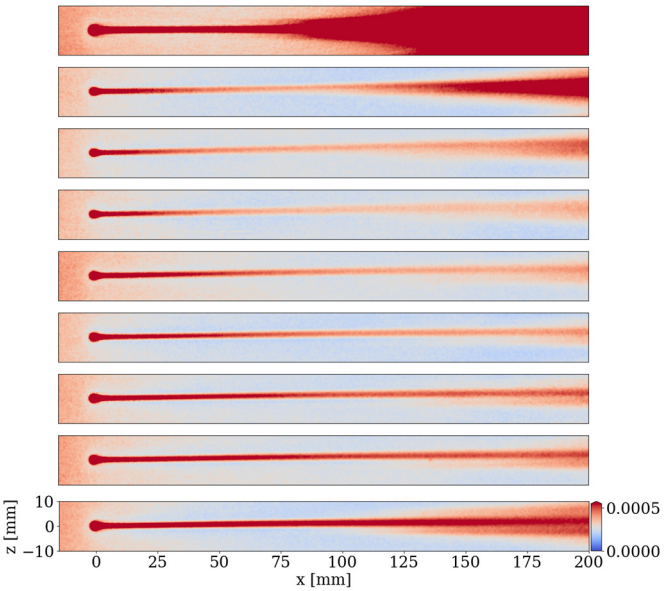

Fig. 6. Distribution of St over the plate surface behind the roughness element (Re group#2, see Table). Blunting radii from top to bottom: 0.0, 0.3, 0.4, 0.5, 0.6, 0.8, 1.0, 1.2, 2.0 mm

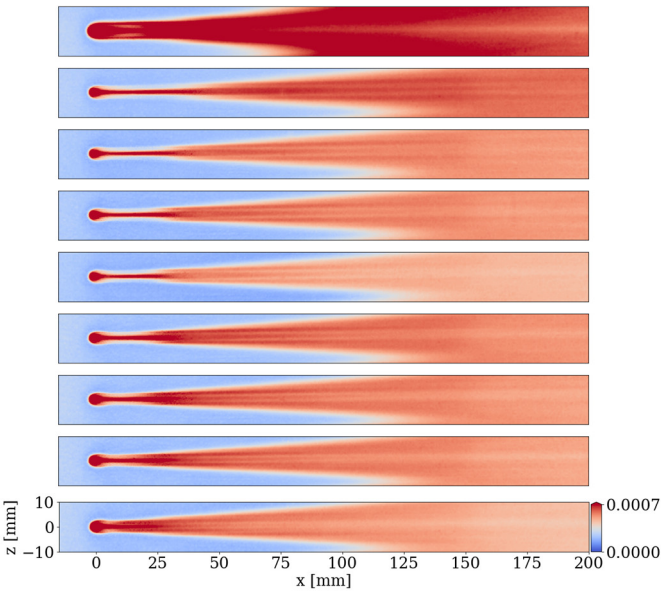

Fig. 7. Same as Fig. 6; Re group #3 (see Table)

One may also note that a central vortex seem to break down for R=0.3 mm, while the reversal trend (R=2.0mm) shows rather solid central vortex with transition starting at its periphery.

Increasing the Reynolds number by the factor of approx. two (#3) and higher (#4), for which the roughness is effective behind the sharp leading edge, does not reveal a reversal trend. The turbulent wedge moves upstream toward the roughness element. This might reflect the fact that only reversed part of the trend takes place at these conditions.

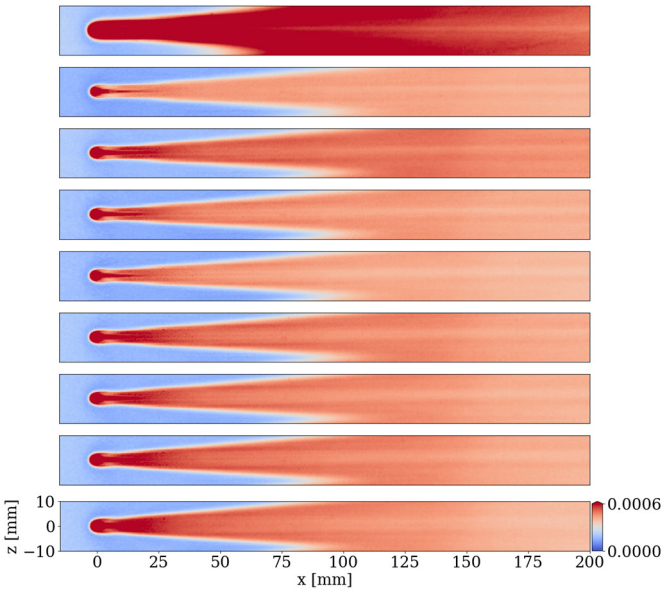

Fig. 8. Same as Fig. 6; Reynolds group #4 (see Table)

The observed behavior shown in Fig. 5–8 is a combined effect of the entropy layer on the roughness-induced transition.

3.3 Bluntness effect

Blunting the leading edge forms the layer of high temperature low-density gas above the surface. To assess the properties of the boundary layer near the roughness element, numerical simulation of several experimental conditions have been performed using in-house software HSFlow [12]. Solutions are obtained by advancing the initially uniform flow field to its steady state. The surface is at constant temperature that corresponds to the experimental conditions. The formulation of the numerical problem is common and omitted here for brevity. The cases of radii R = 0.0, 0.2, 0.4, 0.7, 1.0, 2.0 are computed for every Reynolds group (see Table). In order to extract data for a particular experimental condition, the obtained numerical results are interpolated to the experimental point. The boundary layer thickness δ is found from total enthalpy condition $H(y=\delta)=H_e=0.995H_\infty$. Then displacement thickness is estimated as:

$$\delta^* = \int_0^{1.1\delta} \left(1 - \frac{\rho(y)u(y)}{\rho_e u_e}\right) dy, \qquad (2)$$

where subscript ‘e’ denotes a value on the upper edge of the boundary layer. The factor 1.1 is applied for numerical purposes and weakly affects the resulting value. Note that the enthalpy approach works well in case of bluntness, though it underestimates the boundary layer thickness and consequently the corresponding values of M_e and Re_e in case of sharp leading edge, compared to the $0.99u_\infty$ approach. The edge values should be close to the free-stream ones because viscous-inviscid interaction is weak.

Obtained that way, the edge values are shown in Fig. 9 versus the blunting radius. They drop abruptly at small bluntness that is not captured in the experiments. Then the edge Mach number slowly decreases, while Re_e first attains its local minimum near R=0.5–0.8 mm and then increases with bluntness. The value of Re_e at the largest bluntness R=2.0mm is about 7% larger than its minimum value. This behavior points to the fact that the most stable regime for the roughness-induced transition should occur at some intermediate value of R, because both decrease in M_e and increase in Re_e are known to destabilize the roughness wake.

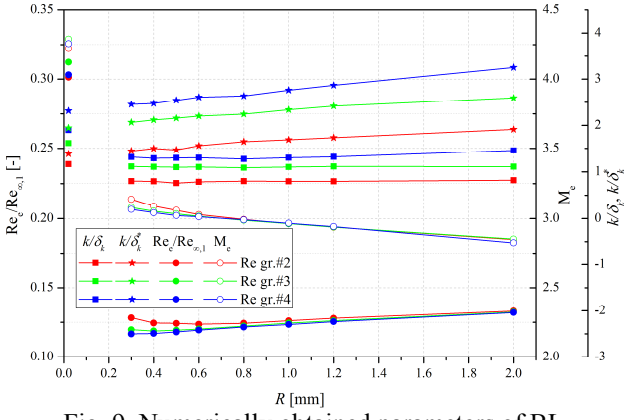

Fig. 9. Numerically obtained parameters of BL depending on the bluntness radius of the leading edge.

The present experiments deal with the roughness element of the fixed height k=1.0 mm. The roughness height-to-BL thickness ratio also varies as radius increases. Though the variation of the value k/δ_k is nearly absent, the value of k/δ_k^* rises noticeably (see Fig. 9). Therefore not only the behavior of M_e and Re_e but also the rising k/δ_k^* with bluntness radius destabilizes the roughness wake. From this point of view, the reversal trend observed for Reynolds group #2 (see Fig. 6) may be attributed to first stabilization of the wake because of dramatic reduction of Re number, its further stabilization due to Re_e decreasing, and then its destabilization due to decreasing M_e and increasing Re_e, k/δ_k^*.

Consider Fig. 10 that shows the dependence of transition onset Reynolds number versus the blunting Reynolds number. The reversal trend discussed above is clearly visualized with the red circles. The Re group #3 show similar though hardly detectable behavior near $Re_b=10^4$. The highest Reynolds number group #4 show monotonically decreasing trend. Note that $Re_{tr,o}$ tends to nearly constant value for #3 and #4 starting from $Re_b\approx5\times10^4$, possibly indicating the effective roughness regime in the presence of bluntness.

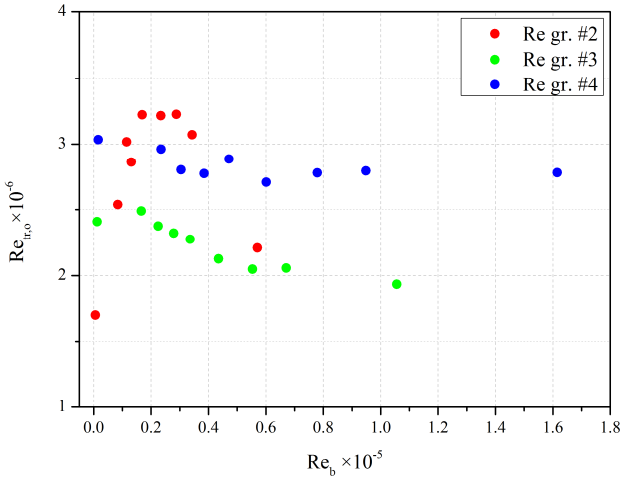

Fig. 10. LTT Reynolds number vs. Re_b

Consider the results of Fig. 10 with respect to the roughness element, which is shown in Fig. 11. The value of $\Delta Re_{tr,o} = Re_{tr,o} - Re_{xk} = Re_{\infty,1} \times (x_{tr,o} - x_k)$ behaves qualitatively similar to $Re_{tr,o}/Re_{\infty,1}$ in Fig. 10. Note that the values of $\Delta Re_{tr,o}$ for Re groups #3 and #4 gather quite close to each other and tend to the constant value when $Re_b>5\times10^4$. The constant $\Delta Re_{tr,eff}=5\times10^6$ was originally proposed for effective roughness element in [13] as being independent on wall cooling. The experiments [13] were done using cones with calibrated microspheres at M_e=2.71, which is rather close to the BL edge conditions for large bluntness radii (approx. 2.8 for the present experiments), i.e. at the bottom of the entropy layer.

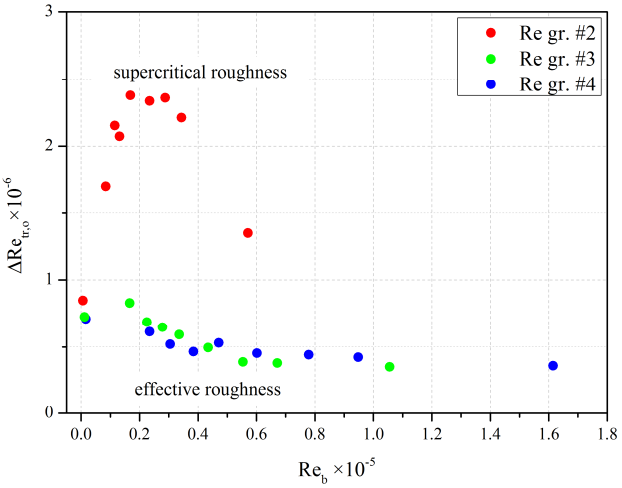

Fig. 11. Roughness-related LTT Reynolds number vs. Re_b

4 Conclusion

Isolated roughness-induced laminar-turbulent transition has been investigated experimentally for a blunt flat-plate Mach 6 flow with roughness element of straight cylindrical shape and of fixed height 1.0 mm located 60 mm downstream from the leading edge, and for four different Reynolds numbers. Eight blunting radii from 0.3 to 2.0 mm have been considered in addition to the sharp leading edge. Experiments have been done in shock wind tunnel UT-1M facility (TsAGI). The transition reversal on the smooth plate has not been observed in the present experiments.

Small bluntness of the leading edge forms an entropy layer above the plate, which results in a drastic drop of Mach (M_e) and Reynolds (Re_e) numbers at the upper edge of the boundary layer. Increasing the radius leads to slow decrease of M_e and decreasing-increasing behavior of Re_e, with roughness height-to-displacement thickness of undisturbed boundary layer rising. For fixed Re_∞ number, rather small bluntness produces a stabilizing effect as the radius increases; thus, the turbulent wedge apex may move downstream away from the roughness element. For bigger

blunting radii, destabilizing effect is observed, when the apex moves back toward the roughness element. The described reversal behavior has been observed experimentally in the present work.

This behavior might be connected to the transition reversal phenomenon that takes place on smooth bodies as the size of their leading edge bluntness increases. The bluntness roughness is hardly controllable, while it could be the major source of reversal. On the contrast, it is much simpler to control the geometry of an isolated roughness element that is located in a thick boundary layer far away from the leading edge.

A sufficiently thick entropy layer decreases the transition Reynolds number based on the free-stream parameters and on the distance from the effective roughness element. This implies the transition station to move upstream toward the roughness element as bluntness becomes larger.

Acknowledgements

The work has been carried out in Central Aerohydrodynamic Institute (TsAGI) under the support of Russian scientific foundation (project no. 17-79-10433). Code for analysis of numerical simulation results in terms of boundary layer properties was developed in TsAGI under the support of Russian Foundation for Basic Research (project no. 16-08-01200) and adapted for the purpose of the present study.

References

[1] Chuvakhov P.V., Egorov I.V., Olivier H., and Roghelia A. Joint Influence of High Entropy Layer and Goertler Vortices on Heat Transfer in Supersonic Compression Ramp Flow. *Computational Thermal Sciences: An International Journal*, Vol. 8, No. 6, pp. 543–553, 2016.

[2] Chuvakhov P.V., Borovoy V.Ya., Egorov I.V., Radchenko V.N., Olivier H, and Roghelia A. Effect of Small Bluntness on Formation of Görtler Vortices in a Supersonic Compression Corner Flow. *Journal of Applied Mechanics and Technical Physics*, Vol. 58, No. 6, pp. 975–989, 2017.

[3] Roghelia A., Chuvakhov P.V., Olivier H., and Egorov I.V. Experimental investigation of Görtler vortices in hypersonic ramp flows behind sharp and blunt leading edges. *47th AIAA Fluid Dynamics Conference*, AIAA Paper 2017-3463, 2017.

[4] Reda D.C. Review and Synthesis of Roughness-Dominated Transition Correlations for Reentry Applications. *Journal of Spacecraft and Rockets*, Vol. 39, No. 2, pp. 161–167, 2002.

[5] Schneider S.P. Effects of Roughness on Hypersonic Boundary-Layer Transition. *Journal of Spacecraft and Rockets*, Vol. 45, No. 2, pp. 193–209, 2008.

[6] McCauley W.D., Saydah A.R., and Bueche J.F. Effect of Spherical Roughness on Hypersonic Boundary-Layer Transition. *AIAA Journal*, Vol. 4, No. 12, pp. 2142–2148, 1966.

[7] Holloway P.F. and Morrisette E.L. Roughness effect on boundary-layer transition for blunt-leading-edge plates at Mach 6. *NASA Technical note,* D-3517, 1966.

[8] Potter J.L. and Whitfield J.D. Effects of slight nose bluntness and roughness on boundary-layer transition in supersonic flow. *J. Fluid Mech.*, Vol. 12, pp. 501, 1962.

[9] Chuvakhov P.V. Controlled experiment on isolated roughness-induced transition in sharp flat plate hypersonic flows. *19th International conference on the methods of aerophysical research (ICMAR 2018)*, Novosibirsk, Russia, pp. 1–10, 2018.

[10] Mosharov V.E. and Radchenko V.N. Measurements of heat flux fields in short-duration wind tunnels by temperature-sensitive paints. *Uch. Zap. TsAGI*, Vol. 38, No. 1-2, pp. 94–101, 2007, in Russian.

[11] Simeonides G.S. Correlation of laminar-turbulent transition data over flat plates in supersonic / hypersonic flow including leading edge bluntness effects. *Shock Waves*, Vol. 12, pp. 497–508, 2003.

[12] Egorov I.V. and Novikov A.V. Direct numerical simulation of laminar–turbulent flow over a flat plate at hypersonic flow speeds. *Computational Mathematics and Mathematical Physics*, Vol. 56, No. 6, pp. 1048–1064, 2016.

[13] Van Driest E.R. and Blumer C.B. Boundary-Layer Transition at Supersonic Speeds – Three-Dimensional Roughness Effects (Spheres). *J. Aerospace Sci.*, Vol. 29, No. 8, pp. 909–916, 1962.

Contact Author Email Address

mailto:pavel_chuvahov@mail.ru

Copyright Statement